Passive Microsensor Based on LC Resonators for Substance Identification

Diego A. Sanz[1], Edgar A. Unigarro[1], Johann F. Osma[1] and Fredy Segura-Quijano[*1]
[1]CMUA. Department of Electrical and Electronics Engineering, Universidad de los Andes
*Corresponding author: Universidad de los Andes, fsegura@uniandes.edu.co (Fredy Segura-Quijano)

Abstract: A scheme for inductive wireless powering and readout of passive LC sensor is presented. The sensor's inductor is designed as a planar square coil and is used as the power-receiving component. The capacitor is connected directly to the inductor and it was designed as an interdigital capacitor (IDC). With a transmitting coil (coupling antenna), an electromagnetic field is generated which couples with the sensor, affecting the impedance of the coupling antenna. This work studies the effects of permittivity variations in a capacitive transducer induced by different solutions. All the fabrication and characterization processes were carried out at the clean room of the Universidad de los Andes. The design and the simulation of the wireless passive micro sensor based on LC resonators were made using the RF module of COMSOL 4.2a.

Keywords: Wireless sensor, passive sensor, electromagnetic field, multiphysics simulation, COMSOL 4.2a.

1. Introduction

Wireless passive sensors have several advantages over wired or active sensors, as they can be placed in places of difficult access or in fragile systems (e.g. inside an organ [1]). These type of sensors have a longer life span, and reduce maintenance costs and complexities [2], while having unexploited benefits to society like a potential reduction of failures [3].

On this work, a wireless passive microsensor, previously designed to measure a wide range of substances, is tested under electromagnetic waves simulation. Different substances are placed on top of the sensor, changing the capacitance of the sensor (Figure 1). A coupling antenna placed at a fixed distance from the sensor is excited with an electrical current at different frequencies, generating electromagnetic fields that induce currents on the sensor. The induced currents on the sensor alter the electromagnetic fields produced by the antenna until the system reaches steady state. The coupling between the sensor and the antenna depend on the geometry of the system. The effect of the substances affects the whole system impedance, which can be measured directly on the coupling antenna. For each substance with different dielectric constant, a unique value of resonance frequency is obtained making possible the identification of each tested substance.

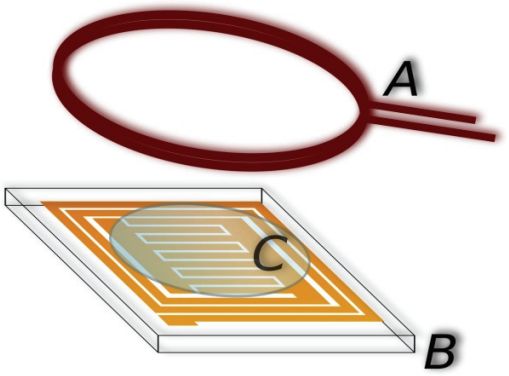

Figure 1. System representation. A is the coupling antenna. B is the sensor and C is the drop of the substance to me meassured.

The purpose of this work, was to simulate different geometry configurations of the coupling antenna to obtain the configuration that maximizes the magnetic coupling between the sensor and the antenna at a fixed distance between them with air as the substance on top of the sensor. With the configuration that maximizes the coupling of the antenna with the sensor, the response of the system in the presence of different substances was studied. By changing the dielectric constant of the substance placed on top of the sensor over a wide range of values, it was intended to verify that the designed sensor was suitable for measuring a wide variety of substances. For these purposes, the RF module of COMSOL V4.2a was used in the frequency domain, to study the system in steady state at different frequencies. With the results obtained, it was possible to determine the configuration that maximized the coupling between the sensor and the antenna. With this

configuration, the resonance frequency of the sensor was extracted for each measured substance. The simulation results were similar to the ones obtained experimentally with a Vector Network Analyzer (VNA) (data not shown).

2. Governing Equations

The propagation of the electromagnetic waves inside dielectric materials, such as air or glass, is described by the following equation on the electric field **E.**

$$\nabla \times \boldsymbol{\mu_r^{-1}}(\nabla \times \mathbf{E}) - \left(\frac{\omega}{c_0}\right)^2 \left(\boldsymbol{\epsilon_r} - \frac{j\sigma}{\omega\epsilon_0}\right)\mathbf{E}=0 \quad (1)$$

In this equation, μ_r, σ *and* $\boldsymbol{\epsilon_r}$ are the relative permeability, the conductance and the relative permittivity of the dielectric material. ω is the angular frequency, c_0 is the speed of light in vacuum and $\boldsymbol{\epsilon_0}$ is the permittivity of free space.

For the domains that present a small penetration of the electromagnetic waves inside them, the electromagnetic waves at the boundary can be estimated by the boundary condition shown in Eq. 2, which takes into account the small penetration or propagation of the electromagnetic waves.

$$\sqrt{\frac{\mu_0\mu_r}{\epsilon_0\epsilon_r - j\frac{\sigma}{\omega}}}\,\mathbf{n}\times\mathbf{H} + \mathbf{E}\text{-}(\mathbf{n}\cdot\mathbf{E})\mathbf{n}=(\mathbf{n}\cdot\mathbf{E_s})\mathbf{n}\text{-}\mathbf{E_s} \quad (2)$$

The excitation of the coupling antenna is made by a lumped port, which relates the electric potential across the port, with its current by the impedance of the port ($Z = \frac{V}{I}$). In the case of a rectangular port, the electromagnetic wave propagation in the lumped port is described with Eq. 3.

$$\mathbf{n}\times(\mathbf{H}_1 - \mathbf{H}_2) + \frac{h}{Zw}\mathbf{n}\times(\mathbf{E}\times\mathbf{n}) = 2\frac{h}{Zw}\mathbf{n}\times(\mathbf{E}_0\times\mathbf{n}) \quad (3)$$

Z is the impedance of the lumped port with dimensions w and h. In this case, $\mathbf{E_0}$ is the incident electric field, while **E** is the total electric field. The term $\mathbf{n}\times(\mathbf{H}_1 - \mathbf{H}_2)$ corresponds to the surface current of the port, which is determined by the difference of the **H** field on each side of the port's boundary.

3. Methods

The whole system is modeled in 3D because there were no symmetry planes due to the geometry of the sensor.

The sensor was designed and later fabricated on 1 mm thick glass substrate, with 120 µm wide and 63 µm thick copper strips with separation between the strips of 75 µm. The total area of the sensor was of 1 cm x 1 cm. The coupling antenna was placed at a fixed distance of 5 mm on top of the sensor. The major radius of the antenna, and the number of turns of the coil were the parameters swept to obtain the maximum coupling between the antenna and the sensor. The thickness of the wire used for the antenna was of 255 µm.

A sphere of air was used to propagate the electromagnetic waves between the sensor and the antenna, and in their surroundings. The outer layers of the sphere were set with Perfectly Matched Layers (PML) to simulate the propagation of the electromagnetic waves to infinity by reducing the reflections of the waves. The sensor was placed in the middle of the sphere with the antenna 5 mm on top of it.

In order to make the simulations more efficient in memory usage and in computational load, the metallic domains were not taken into account completely. Only their external boundaries were taken into account, and the Impedance Boundary Condition of the RF module was used for them. This boundary condition satisfies Eq. 2. The lumped port is set with a terminal current of 1 A.

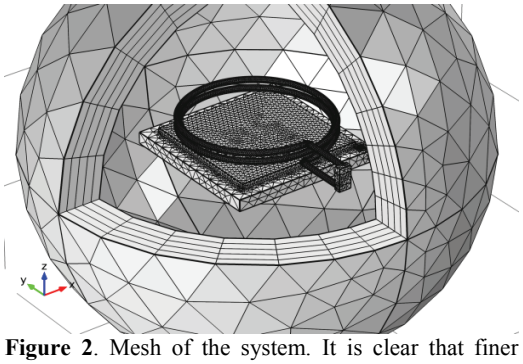

Figure 2. Mesh of the system. It is clear that finer elements are found in the middle of the sphere while coarser elements are found on the sphere's boundary.

Each domain of the model was meshed separately, in order to have finer elements in the center of the sphere and coarser at the PML (Figure 2).

4. Theory

4.1 Coupling Optimization

In order to model the coupling of the antenna with the sensor, the magnetic linear coupling parameter k can be taken into consideration. In this approximation, a strong coupling happens when k has a magnitude of 1. In this case the sensor's resonance frequency is highly affected by the coupling antenna's own resonance frequency which is not desired. As the sensor and the antenna were separated by 5 mm, the coupling between them was small in magnitude. In this case, a good coupling is the one that maximizes the Q-factor of the resonator corresponding to the sensor. In Eq. 4 the Q factor is calculated as the ratio between the resonance frequency and the bandwidth of the resonator. Variations of 1, 2 and 3 turns in the coil and different outer radius of the antenna were evaluated.

$$Q = \frac{f_r}{\Delta f} \qquad (4)$$

4.2 Substances Measurements

As the dielectric constant of the substance on top of the sensor increases, the capacitance of the sensor is expected to increase. This causes a decrease in magnitude on the resonance frequency of the sensor. At the same time, the peak of the sensor's resonator is expected to decrease, because the sensor becomes more capacitive, storing more energy in the electric field and less in the magnetic field, which is the one that affects directly the coupling antenna. For the purposes of this work, a good design on the sensor is the one that always presents a resonator for any dielectric constants chosen within the range chosen for the design. The sensor was designed to work from 1 to 80.1 in the dielectric constant of the substance placed on top of the sensor, with all the resonance frequencies below 75 MHz.

5. Simulation Results

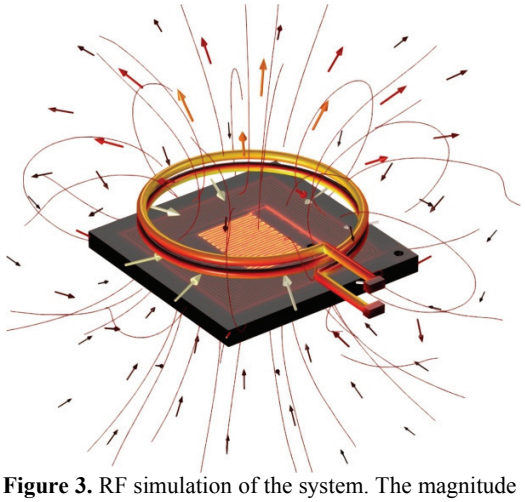

Figure 3. RF simulation of the system. The magnitude of the electric field is shown on the top surface of the sensor. In the middle of this surface, where the IDC is located, the largest magnitude of electric field is obtained, as it was expected. The magnetic field magnitude is shown on the surface of the coupling antenna. Magnetic field lines and arrows are shown as they pass through the sensor and the antenna making showing where the magnetic coupling between them originates.

5.1 Coupling Optimization

Figure 4 shows some of the results obtained for the same resonator under different geometries of the coupling antenna.

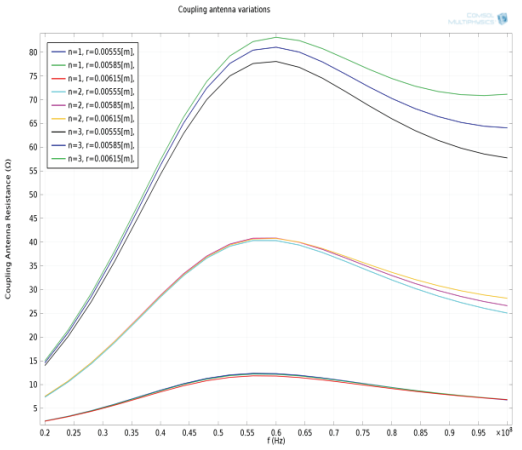

Figure 4. Some simulation results for different radius of the antenna, for 1, 2 and 3 turns of the antenna's coil. Each curve (resonator) is the result of the simulation with air as the substance on top of the

sensor, for a certain number or turns and a specific radius on the antenna.

5.2 Substances Measurements

The results obtained for substances with dielectric constants of 1, 6.2, 13.26, 38.25 and 80.1 are shown on Figure 5.

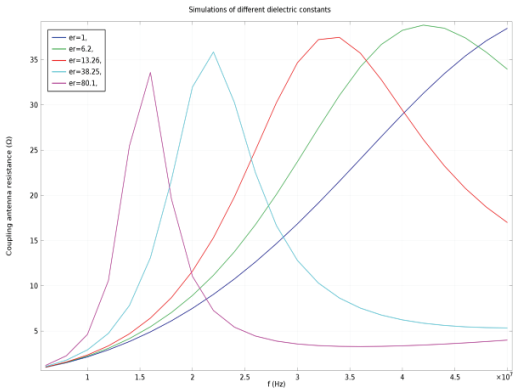

Figure 5. Real part of the Impedance of the system for different substances placed on top of the sensor. The substances' dielectric constants are 1, 6.2, 13.26, 38.25 and 80.1.

6. Discussion

In Figure 4, it can be appreciated that the resonators sensibility with the outer radius of the antenna, is small. As for the variations on the number of turns of the coil, considerable changes on the resonators shape and magnitude are appreciated. After eliminating the background signal so that the resonators tend to 0 in $\pm\infty$, the Q-factor of the resonators is calculated (see Eq. 4). The configuration that maximized the Q-factor of the sensor's resonator was the antenna with a 2-turns coil and an outer radius of 5.85 mm.

The results shown on Figure 5 indicate that all the resonators, which correspond to each substance, can be easily identified. It also shows that the resonance frequency for each case can be extracted. Some of the chemicals associated with the simulated dielectric constants are: air (1), pyridine (13.26) and Milli-Q water (80.1). The results of the simulations are similar with the measures taken with a VNA on fabricated sensors at the Sala Limpia (Clean room) of Universidad de los Andes (data not shown). The major difference was that on experimental results, the peaks decrease more significantly with the increase of the dielectric constant, than in the simulation results.

7. Conclusions

It was possible to determine the best geometric parameters of the coupling antenna to maximize the coupling between the antenna and the sensor using full 3D simulation of the system.

In the other hand, the designed sensor proved to be suitable to measure a wide range of dielectric constants that correspond to different substances.

8. References

1. Po-Jui Chen; Dodger, D.C.; Saati, S.; Humayun, M.S.; Yu-Chong Tai, "Microfabricated Implantable Parylene-Based Wireless Passive Intraocular Pressure Sensors," *Microelectromechanical Systems, Journal of*, **Volume 17, no. 6**, pp.1342-1351 (2008)

2. K. Ong; J. Wang; R. Singh; L. Bachas; C. Grimes, "Monitoring of bacteria growth using a wireless, remote query resonant-circuit sensor: application to environmental sensing," *Biosensors and Bioelectronics*, **Volume 16**, 4-5 (2001)

3. G. Stojanovic; M. Radovanović, M. Malešev, V. Radonjanin, "Monitoring of water content in building materials using a wireless passive sensor," *Sensors*, **Volume 10 (5)**, pp. 4270-4280 (2010)

9. Acknowledgements

This project was possible thanks to the collaboration of the MOX - Center of Advanced Computing – Faculty of Engineering, Universidad de los Andes for providing the computational resources.